DOI:10.2478/10004-1254-63-2012-2202

Scientific paper

GLUTATHIONE CONJUGATES OF OCHRATOXIN A AS BIOMARKERS OF EXPOSURE*

Mariana TOZLOVANU[1,§] Delphine CANADAS[1], Annie PFOHL-LESZKOWICZ[1], Christine FRENETTE[2,§], Robert J. PAUGH[2], and Richard A. MANDERVILLE[2]

Laboratory of Chemical Engineering, Department of Bioprocess and Microbial System, UMR CNRS/INPT/UPS 5503, ENSA Toulouse, France[1], Departments of Chemistry and Toxicology, University of Guelph, Guelph, Ontario, Canada[2]

Received in January 2012
CrossChecked in August 2012
Accepted in March 2012

In the present study the photoreactivity of the fungal carcinogen ochratoxin A (OTA) has been utilised to generate authentic samples of reduced glutathione (GSH) and *N*-acetylcysteine (NAC) conjugates of the parent toxin. These conjugates, along with the nontoxic OTα, which is generated through hydrolysis of the amide bond of OTA by carboxypeptidase A, were utilised as biomarkers to study the metabolism of OTA in the liver and kidney of male and female Dark Agouti rats. Male rats are more susceptible than female rats to OTA carcinogenesis with the kidney being the target organ. Our studies show that the distribution of OTA in male and female rat kidney is not significantly different. However, the extent of OTA metabolism was greater in male than female rats. Much higher levels of OTα were detected in the liver compared to the kidney, and formation of OTα is a detoxification pathway for OTA. These findings suggest that differences in metabolism between male and female rats could provide an explanation for the higher sensitivity of male rats to OTA toxicity.

KEY WORDS: *bioactivation, carcinogenicity, DNA adduction, glutathione, metabolism, mutagenicity, N-acetylcysteine*

Ochratoxin A (OTA, Figure 1) is a mycotoxin produced by several fungi of *Aspergillus* and *Penicillium* species (1-5). It consists of a chlorophenolic group containing a dihydroisocoumarin moiety that is amide-linked to phenylalanine. The toxin is a common contaminant of cereals and agricultural products (2, 3), and the International Agency for Research on Cancer (IARC) has classified OTA as a possible human carcinogen (group 2B) (6). OTA is nephrotoxic and is a potent renal carcinogen in rats (7) and in chicks (8). In humans, OTA has been associated with nephropathies in the Balkans (9) and in North African countries (10).

Because OTA is a possible human carcinogen present in food products, tolerable daily intakes (TDIs) are proposed by government agencies to manage the risk of OTA exposure. The TDI for OTA established by the Joint FAO/WHO Expert Committee on Food Additives has been set at ~ 14.28 ng kg^{-1} b.w. per day (100 ng kg^{-1} b.w. per week), based on nephrotoxic effects in pigs (11). Health Canada has proposed a TDI of 4 ng kg^{-1} b.w. per day that considers tumour formation by OTA (5). These differences in TDI stem from a lack of consensus concerning the mechanism

* The subject of this article has partly been presented at the International Symposium "Power of Fungi and Mycotoxins in Health and Disease" held in Primošten, Croatia, from 19 to 22 October 2011.
§ These authors contributed equally to this work.

of action (MOA) for OTA. However, Hibi et al. (12) have recently demonstrated the *in vivo* mutagenicity of OTA in male rat kidney, suggesting involvement of a direct genotoxic mechanism in OTA-mediated renal carcinogenesis. The more stringent TDI proposed for OTA by Health Canada is more in line with carcinogens whose MOA involves direct genotoxicity (5).

Direct genotoxicity by OTA may stem from its oxidative metabolism into electrophiles that are capable of reacting covalently with DNA to generate DNA adducts (13, 14). OTA possesses a chlorophenolic group, and chlorophenols are well known to undergo oxidative dechlorination reactions to afford quinone/hydroquinone redox couples (15, 16). The hydroquinone metabolite (OTHQ, Figure 1) of OTA has been detected in the urine (17) and kidneys (18) of rats, and in human blood and urine samples (19). Oxidation of OTHQ generates the quinone electrophile OTQ that reacts with DNA to generate covalent DNA adducts, as evidenced using ^{32}P-postlabeling (20). OTA also reacts photochemically with 2′-deoxyguanosine (dG) to generate a carbon (*C*)-linked nonchlorinated ochratoxin B (OTB)-dG adduct (21) that has recently been detected in the kidney of male rats using liquid chromatography-mass spectrometry (LC-MS) (22). The C5-Cl atom of OTA plays a critical role in OTB-dG formation, as the nonchlorinated OTB analog lacks direct genotoxicity and does not react photochemically with dG to generate the OTB-dG adduct (23).

The C5-Cl atom of OTA also plays a role in its metabolism by carboxypeptidase A into the nontoxic ochratoxin a (OTα, Figure 1) and phenylalanine. The nonchlorinated OTB derivative undergoes hydrolysis by carboxypeptidase A at a faster rate than OTA (24, 25) and this has been invoked as a rationale for the lower toxicity of the OTB analog (26). The nontoxic OTα has previously been detected as the major OTA metabolite in human blood and urine samples (27) and may serve as a sensitive biomarker for OTA exposure (28). Other biomarkers for OTA exposure would include the OTB-dG adduct (22), as OTA is mutagenic (12), and OTB-dG formation suggests that a reactive metabolite of OTA has reached a toxicologically significant target (DNA). However, the presence of OTB-dG in treated rat kidney samples is low, 20 to 70 per 10^9 nucleotides (22). Furthermore, the adduct OTB-dG is unstable and undergoes hydrolysis in the presence of acid, which is commonly used for OTA extraction from biological and food samples (27, 29). These traits (low abundance and poor stability) make OTB-dG unsuitable as a general biomarker for OTA exposure.

Electrophiles generated from the metabolism of OTA also react with reduced glutathione (GSH) to produce GSH-conjugates. The OTB-GSH conjugate (Figure 1) is the major species formed from the photoreaction of OTA with excess GSH (23) and corresponds structurally with OTB-dG. Nucleophilic

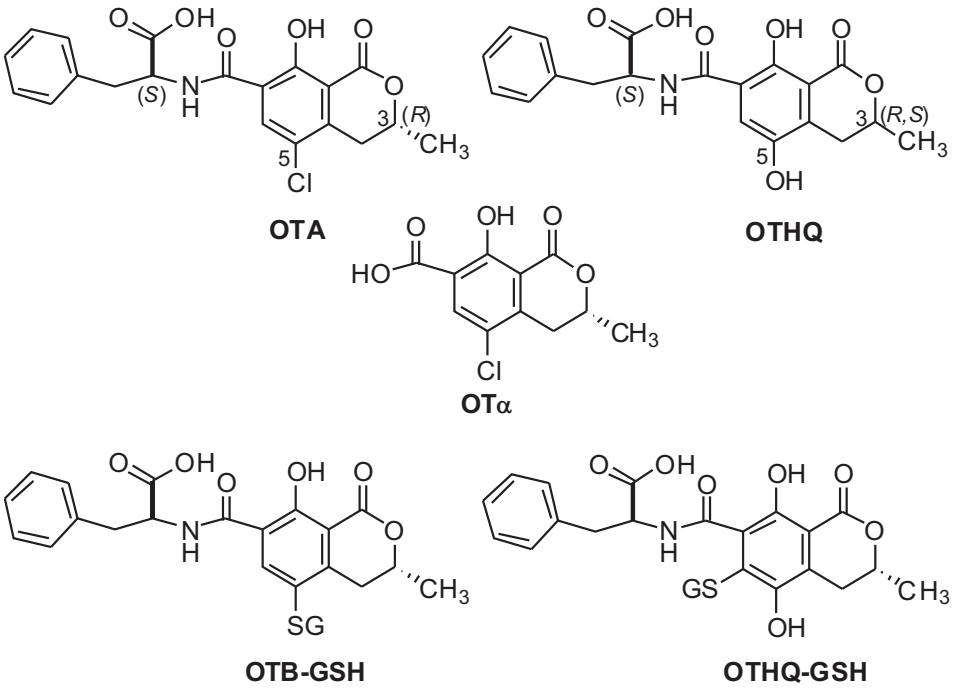

Figure 1 *Chemical structures of OTA and OTA metabolites.*

attachment of GSH to the quinone electrophile OTQ affords OTHQ-GSH (Figure 1) that has been characterised previously using NMR spectroscopy and is generated by treatment of OTA with rat liver microsomes in the presence of excess GSH (30). Unlike the DNA adduct OTB-dG, OTB-GSH and OTHQ-GSH are stable to acid treatment and can be extracted from biological samples using methodology established for extraction of the parent toxin OTA (27, 29).

In the present study authentic samples of OTB-GSH, OTHQ-GSH, and the corresponding *N*-acetylcysteine (NAC) conjugates of OTA have been used as biomarkers to examine OTA metabolism in the liver and kidney of male and female rats. Our goal was to use the conjugates to determine sex and organ differences in OTA metabolism, given that the male rat is particularly susceptible to OTA-mediated carcinogenesis, with the kidney being the target organ (7). Our studies provide new evidence for OTB-GSH and OTHQ-GSH formation in liver and kidney of both sexes. Interestingly, clear differences in the extent of OTB-GSH *versus* OTHQ-GSH formation was observed in male *versus* female and liver *versus* kidney, with the male kidney providing preferential OTB-GSH formation. These findings may help shed light on the susceptibility of male rats to OTA-mediated carcinogenesis.

MATERIALS AND METHODS

Materials

OTA (benzene free, CAS# 303-47-9) was purchased from Sigma (Saint Quentin Fallavier, France). A synthetic sample of OTHQ (30) was available in the laboratory at Guelph, Canada, and was used as a mixture of diastereomers [3(R, S)], (Figure 1). Stock solutions of OTA and OTHQ in aqueous 50 mmol L^{-1} phosphate buffer pH 7.4 were prepared as outlined previously (31, 32). Glutathione (GSH) and N-acetylcysteine (NAC) were purchased from Sigma-Aldrich (Oakville, ON, Canada). All HPLC solvents were of chromatography grade and water used for buffers was obtained from a MilliQ filtration system (18.2 MW).

Synthesis of GSH and NAC Conjugates

Authentic samples of GSH and NAC conjugates of OTA were generated from the photoreaction of OTA or OTHQ with GSH or NAC. Reaction mixtures (2 mL total volume) of 1 mmol L^{-1} OTA or OTHQ in the presence of 15 molar equivalent GSH or NAC were irradiated at 350 nm using a Rayonet Chamber Reactor, model RPR-200, as outlined for the synthesis of OTB-GSH and OTHQ-GSH (23). The photoreaction of OTA in the presence of GSH or NAC was used for the generation of OTB-GSH or OTB-NAC, while the corresponding photoreaction of OTHQ with GSH or NAC was used for the preparation of OTHQ-GSH or OTHQ-NAC. Purifications were performed using an Agilent 1200 series HPLC equipped with an autosampler, autocollector, diode array detector (monitored at 258 nm and 340 nm) and fluorescence detector [excitation (λ_{ext}) = 340 nm; emission (λ_{em}) = 465 nm]. Separations were carried out using an Agilent C18 column (150 mm x 4.6 mm, particle size 5 μm) with the following mobile phase: 0.1 % formic acid in H_2O:0.1 % formic acid in acetonitrile (70:30) to (25:75) in 17 min by a linear gradient at a flow rate of 0.75 mL min^{-1}. The GSH- and NAC-conjugate peaks were combined and lyophilised to dryness using a Labconco FreeZone$^{4.5}$ freeze-dry system. The authentic conjugate samples were checked for purity through HPLC analysis (>96 % based on integration of the HPLC trace) and were characterised by MS. Mass spectra were obtained using an Agilent 1100 LC-MSD with a single quadrupole detector with electrospray negative ionisation (ESI^-). The OTB-NAC conjugate was also characterised by nuclear magnetic resonance (NMR) spectroscopy on a Bruker Avance 600 MHz NMR spectrometer equipped with a HCN pulsed-field gradient cryoprobe. Data collection was carried out at room temperature in $^2H_6$-dimethyl sulfoxide, DMSO-d_6 (99.9 %) in a 2 mm NMR tube. The ^1H NMR spectrum was acquired using 1024 scans and a sweep width of 10 ppm. The two-dimensional ^1H-^1H correlation (COSY) spectrum was collected with 2048 complex points in t_2, 512 points in t_1, and 64 transients per t_1 increment. Data were multiplied with optimised phase-shifted squared sinebell apodization functions with zero filling to 1024 points in the t_1 dimension. Spectra were referenced to the DMSO-d_5H peak at 2.50 ppm and were processed using the Topspin 2.1 software (Bruker BioSpin Ltd., Milton, Canada).

Rat tissue samples

Dark Agouti rat lung, liver, and kidney samples were available in the laboratory at Toulouse, France and were obtained from a rat study performed by CIT (International Centre of Toxicology, Evreux) in compliance with the Principles of Good Laboratory Practice as described in: (*i*) OECD Principles on Good Laboratory Practice (revised in 1997), ENV/MC/CHEM (98) 17 and (*ii*) Commission Directive 1999/11/EC of 8th March 1999 adapting to technical progress the Principles of Good Laboratory Practice as specified in the Council Directive 87/18/EEC on the harmonisation of laws, regulations and administrative provisions relating to the application of the Principles of Good Laboratory Practice and the verification of their applications for tests on chemical substances (OJ No. L 77 of 23rd March 1999). The rat study was modelled after the protocol described in depth in the paper by Castegnaro et al. (27). In the current study, 7-week-old Dark Agouti rats were fed wheat contaminated with various concentrations of OTA over a 28-day period. The rats (25 males and 25 females) were housed in individual cages (43 cm x 21.5 cm x 20 cm) and kept in environmentally controlled conditions (ventilation, 22°C, 12 h dark/light cycles). The wheat provided by the French miller (Paulic Minotiers) was of a common variety used for making bread. All rats had free access to non-contaminated wheat over a 7-day acclimation period. This was followed by exposure of the rats to OTA-contaminated wheat. One batch of 8 kg was coded as control. Four batches, 8 kg each, were artificially contaminated with OTA, respectively at: 2.5 μg kg^{-1}, 7 μg kg^{-1}, 40 μg kg^{-1}, and 100 μg kg^{-1}. To uniformly incorporate OTA into the wheat, OTA was dissolved in ethanol and introduced into the wheat (in the presence of 1 % water) as a fine spray over a 15-min period. Each batch of 8 kg wheat was distributed into 53 plastic bags, each containing 150 g of wheat. The plastic bags were stored at -20 °C in closed plastic containers and were allowed to thaw at room temperature 1 day prior to use. The OTA content of the wheat samples was confirmed using HPLC with fluorescence detection (29). On completion of the treatment period, the rats were euthanised and the organs were weighed and frozen at – 80 °C until use.

OTA and metabolite extraction

OTA and its metabolites were extracted from the organ tissue samples using a procedure similar to the one outlined by Molinié et al. (29) for the extraction of OTA from cereals and modified by Pfohl-Leszkowicz et al. (33). Tissue samples (1 g) were homogenised in the presence of 20 mL 0.1 mol L^{-1} $MgCl_2$ and 0.05 mol L^{-1} HCl (pH 1.5). The aqueous acidic solution was then extracted three times with $CHCl_3$ (20 mL, 10 mL, 10 mL). Following each $CHCl_3$ treatment, the samples were centrifuged (10 min, ~3,000 x *g*, 4 °C) in order to separate the $CHCl_3$ component from the acidic aqueous phase. The combined $CHCl_3$ extracts were then treated with 40 mL sodium bicarbonate and the solution was shaken for ~ 10 min. The bicarbonate solution was collected and acidified to pH 1.5 with HCl and then extracted three times (3 x 20 mL) with $CHCl_3$. The combined $CHCl_3$ extracts were dried under vacuum and the resulting residue was dissolved in 1 mL methanol, filtered, and concentrated under nitrogen to a final volume of 200 μL.

OTA and OTA metabolite analysis

Reverse-phase HPLC analysis of OTA and its metabolites were carried out using a Gilson 811B dynamic HPLC pump. OTA was analysed using a Nucleosil 100-3 C18 column (150 mm x 4.6 mm, particle size 3 mm) under isocratic elution (methanol, 600 mL; acetonitrile, 600 mL; water, 800 mL; sodium acetate, 0.68 g; glacial acetic acid, 28 mL) with detection performed with a programmable fluorimeter GTI spectrovision (λ_{ext}=340 nm; λ_{em}=465 nm). The limit of detection (LOD) was 0.05 ng g^{-1}; the limit of quantification (LOQ) was 0.2 ng g^{-1} (34). The OTA metabolites were separated using a Prontosil C18 column (250 mm x 4 mm, particle size 3 μm) with solvent A: methanol:acetonitrile:6.5 mmol L^{-1} ammonium formate (200:200:600) adjusted to pH 3 with formic acid; and solvent B: methanol: acetonitrile:6.5 mmol L^{-1} ammonium formate (350:350:300) adjusted to pH 3 with formic acid, using gradient elution, as outlined previously (34, 35). Detection was also performed using the fluorimeter GTI spectrovision (λ_{ext}=340 nm; λ_{em}=465 nm) that permitted a LOD of ~ 0.05 ng g^{-1} for OTA.

RESULTS

Generation of GSH and NAC conjugates

The photoreaction of OTA or OTHQ in the presence of 15 molar equivalent GSH or NAC was

utilised to generate the GSH- and NAC-conjugates of OTA. As outlined previously (23), photoirradiation (15 min) of OTA (1 mmol L^{-1}) at 350 nm in the presence of excess GSH generates OTB-GSH (Figure 1) as the major product. The conjugate has a phenolic absorption at l_{max} = 331 nm and a parent ion at *m/z* 673. In the negative ESI spectrum a major fragment ion is observed at *m/z* 400, which is 32 mass units heavier than OTB (*m/z* 368) and stems from b-elimination of the attached benzoquinol-SH (23). The photoreaction also generates OTHQ-GSH (Figure 1) as a minor product (23) that forms by nucleophilic attachment of GSH to the quinone electrophile OTQ (30). This conjugate is the sole species formed from the photoreaction of OTHQ (1 mmol L^{-1}) with excess GSH. It has been fully characterised previously using NMR spectroscopy and possesses a phenolic absorption at l_{max} = 352 nm and a parent ion at *m/z* 689 with a prominent fragment ion at *m/z* 416 from b-elimination of benzoquinol-SH (23, 30).

Figure 2 shows the ESI^- spectra of the corresponding NAC-conjugates of OTA (OTB-NAC) and OTHQ (OTHQ-NAC). The OTB-NAC conjugate had a phenolic absorption at 331 nm and a parent ion at *m/z* 529 with a major fragment at *m/z* 400 (Figure 2A), as noted for fragmentation of OTB-GSH. The phenolic absorption of OTHQ-NAC occurred at 360 nm and the conjugate had a parent ion at *m/z* 545 with a major fragment at *m/z* 416 (Figure 2B). Spectral data for OTA, OTHQ and the corresponding GSH- and NAC-conjugates are given in Table 1.

The OTB-NAC conjugate was also characterised by NMR spectroscopy. Figure 3 shows the two-dimensional ^1H-^1H correlation (COSY) spectrum of

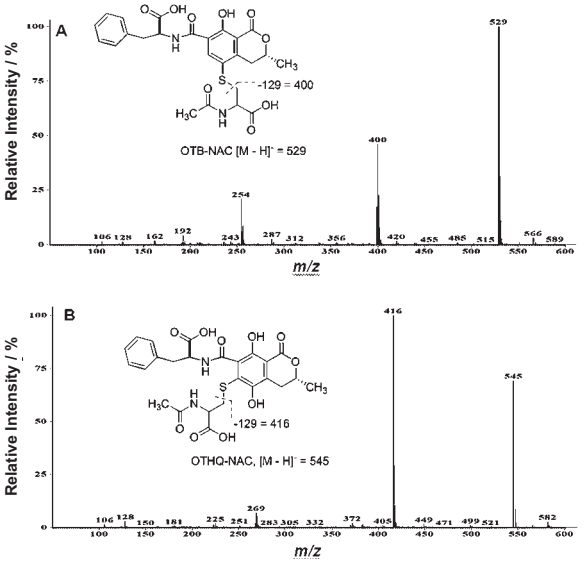

Figure 2 *Negative ionisation electrospray mass spectra of (A) OTB-NAC and (B) OTHQ-NAC.*

the conjugate recorded in DMSO-d_6 at room temperature. The ^1H chemical shifts of the conjugate are given in Table 2. The Table also includes ^1H chemical shift data for OTHQ, which was also recorded in DMSO-d_6 (16), and OTA, which was recorded in $CDCl_3$ by Dais et al. (36). The NMR data together with the MS data provided an unambiguous assignment of the OTB-NAC structure, as ^1H signals for the attached NAC moiety could be determined and H-6 of the OTB component was observed at ~ 8 ppm, as expected from the ^1H NMR data for OTHQ (16) and OTA (36).

Table 1 *Spectral data for photoreactions of OTA and OTHQ with GSH and NAC*[a]

species	RT[c]	λ_{max} [d]	parent ion m/z	fragment ions m/z
OTA[b]	13.3	333	402	358, 314
OTHQ[b]	10.9, 11.0	350	384	340, 296
OTB-GSH[b]	6.8	331	673	672, 544, 400
OTHQ-GSH[b]	6.2	352	689	688, 560, 416
OTB-NAC	9.5	331	529	400
OTHQ-NAC	8.0, 8.2	360	545	416

[a] *Photoreactions of ochratoxins (1 mmol L^{-1}) in the presence of 15 molar equivalent GSH or NAC were carried out in 50 mmol L^{-1} phosphate buffer pH 7.4 for 15 min with irradiation at 350 nm using a Rayonet Chamber Reactor, Model RPR-200.*
[b] *Data taken from reference 23.*
[c] *Retention time in minutes using an Agilent C18 (150 mm x 4.6 mm, 5 mm particle size) column with a flow rate of 0.75 mL min^{-1} using the following mobile phase: 0.1 % formic acid in H_2O:0.1 % formic acid in ACN (70:30) to (25:75) in 17 min by a linear gradient.*
[d] *Phenolic ring absorbance in nm.*

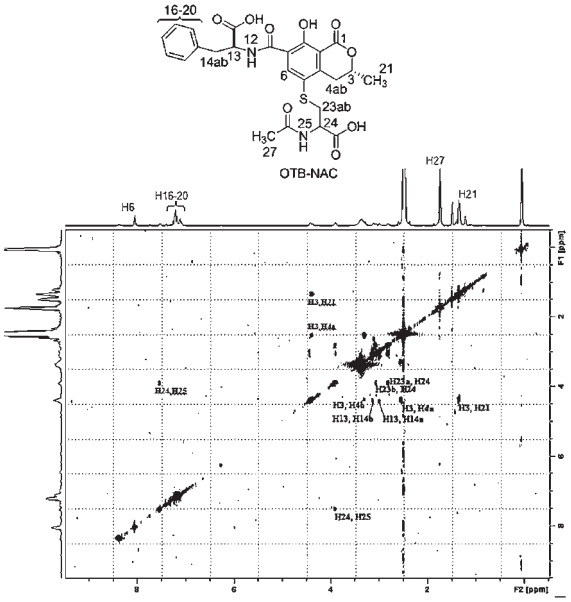

Figure 3 *^{1}H-^{1}H COSY spectrum of OTB-NAC recorded at 600 MHz in DMSO-d_6.*

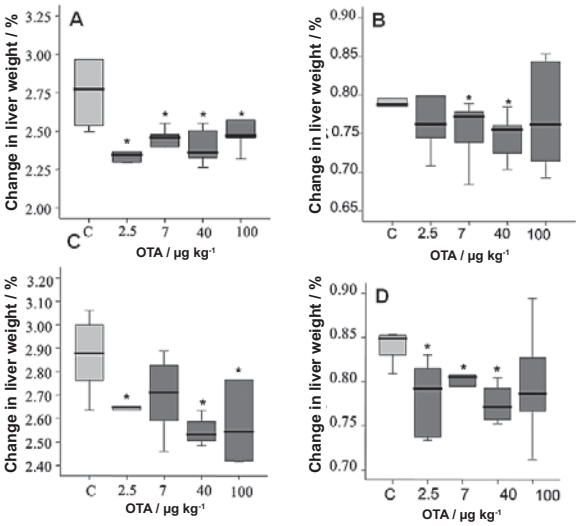

Figure 4 *Change in liver (A, C) and kidney (B, D) weight of male (A, B) and female (C, D) Dark Agouti rats following varying levels of OTA exposure for 28 days.*

Rat studies

From the rat study it was noted that the weight gain of both male and female Dark Agouti rats was unaffected by the level of OTA ingestion (2.5 µg kg^{-1}, 40 µg kg^{-1}, and 100 µg kg^{-1}) following the 28-day period. Figure 4 shows the corresponding changes in liver and kidney weight for males and females. A significant decrease ($p<0.01$, Student t-test) in male (A) and female (C) liver weight was observed for all rats receiving OTA, regardless of concentration, compared to the control (C in the x-axis). This was not the case for the kidney weight (B, D). For both males (B) and females (D), the highest dose (100 µg kg^{-1}) of OTA did not significantly affect the kidney weight compared to the control, even though using Wilcoxon rank test a significant decrease was observed with lower doses.

Table 2 *Proton NMR data for OTB-NAC, OTHQ and OTA.*

proton	δ ^{1}H OTB-NAC[a]	δ ^{1}H OTHQ[b]	δ^{1}H OTA[c]
H-3	4.39	4.29	4.69
H-4a	3.35	3.12	3.22
H-4b	2.55	2.66	2.79
H-6	8.06	7.72	8.36
H-13	4.43	4.29	4.96
H-14a	3.12	3.12	3.30
H-14b	3.08	3.12	3.15
H-16-20 (phenyl)	7.19 to 7.23	7.29	7.13 to 7.30
H-21 (CH_3)	1.34	1.43	1.53
H-23a	3.06	_	_
H-23b	2.81	_	_
H-24	3.91	_	_
H-25 (NH)	7.53	_	_
H-27 (CH_3)	1.75	_	_

[a] *^{1}H NMR chemical shifts in ppm recorded at 600 MHz in DMSO-d_6.*
[b] *Chemical shift data taken from reference 16, recorded at 300 MHz in DMSO-d_6.*
[c] *Chemical shift data taken from reference 36, recorded at 400 MHz in $CDCl_3$.*

Figure 5 shows the distribution of OTA in the lung, liver, and kidney of male (A) and female (B) Dark Agouti rats following varying levels of OTA exposure for the 28-day period. The levels of OTA (ng g^{-1}) presented in Figure 5 were obtained following OTA extraction from the tissues and performing HPLC analysis with fluorescence detection (excitation 340 nm, emission 465 nm), using an authentic sample of OTA for comparison for an LOD of 0.05 ng g^{-1} and an LOQ of 0.2 ng g^{-1}. The relative levels of OTA in the tissues of both sexes were similar to the highest levels being found in the lung and liver. The OTA amounts in different tissues increased with OTA dose.

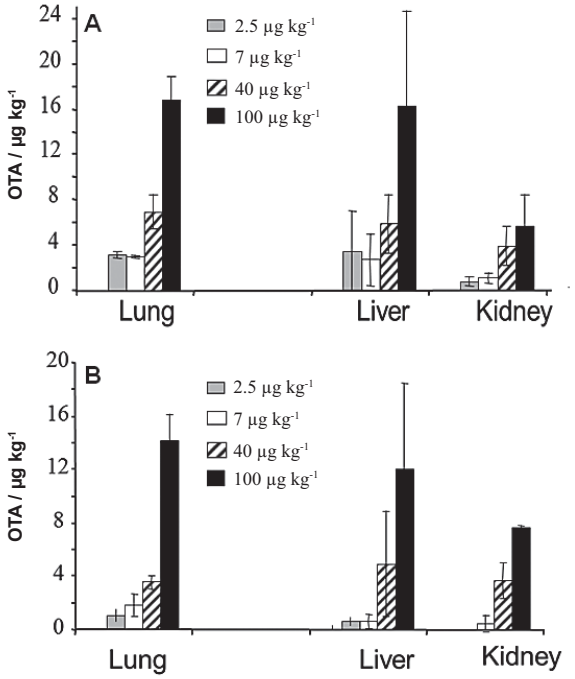

Figure 5 *Distribution of OTA in tissues of male (A) and female (B) Dark Agouti rats following varying levels of OTA exposure for 28 days.*

For rats receiving the highest dose (100 µg kg^{-1}) of OTA, tissue samples were also analysed for metabolite formation using authentic samples of OTa, OTB-GSH, OTHQ-GSH, OTB-NAC, and OTHQ-NAC for comparison. For these studies, OTA and its metabolites extracted from four liver and four kidney samples from each sex were combined for HPLC analysis with fluorescence detection (excitation 340 nm, emission 465 nm) after gradient separation. Figure 6 shows a representative HPLC chromatogram depicting the relative levels of OTA, OTα, OTB-GSH, and OTHQ-GSH from male (A) and female (B) liver samples, while the corresponding HPLC chromatograms from the analysis of the male (A) and female (B) kidney samples are shown in Figure 7. In both tissue samples peaks corresponding to the NAC-conjugates were not observed. However, peaks that co-migrated with OTα and the GSH-conjugates were found. Compared to the peak for OTA, levels of metabolite formation were greater for males (A) than females (B) in both liver (Figure 6) and kidney (Figure 7). The most striking difference between kidney and liver in both sexes was the high degree of OTB-GSH formation in the kidney relative to OTα and OTHQ-GSH. The liver of both sexes generated higher levels of OTHQ-GSH, and relatively high levels of OTα were also detected in male rats (Figure 6A).

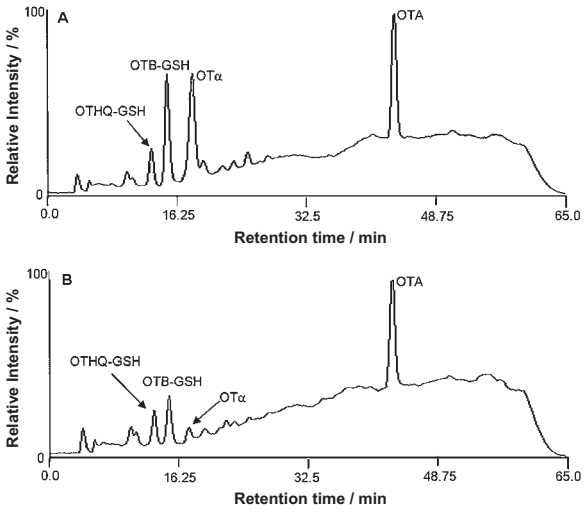

Figure 6 *HPLC chromatograms with fluorescence detection (excitation 340 nm, emission, 465 nm) showing relative levels of OTA, OTα, OTB-GSH and OTHQ-GSH from male (A) and female (B) livers (4 from each sex) following treatment with 100 µg kg^{-1} OTA for 28 days.*

DISCUSSION

The results of our studies highlight the potential utility of GSH- and NAC-conjugates of OTA and OTHQ as biomarkers for OTA exposure. The photoreaction of OTA in the presence of excess GSH (23) or NAC can be used to readily generate authentic samples of OTB-GSH, OTHQ-GSH (Figure 1), or OTB-NAC and OTHQ-NAC (Figure 2). The OTHQ-GSH conjugate stems from the attachment of GSH to the quinone (OTQ) electrophile, which is produced by cytochrome P450 metabolism of OTA (16, 20). The OTB-GSH or OTB-NAC conjugates are generated

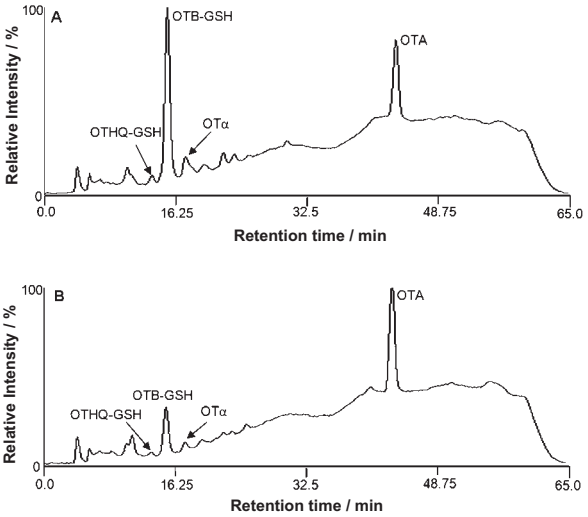

Figure 7 *HPLC chromatograms with fluorescence detection (excitation 340 nm, emission, 465 nm) showing relative levels of OTA, OTα, OTB-GSH and OTHQ-GSH from male (A) and female (B) kidneys (4 from each sex) following treatment with 100 μg kg^{-1} OTA for 28 days.*

photochemically from displacement of the C5-Cl atom of OTA by the sulphur atom of GSH or NAC. The electrophilic intermediate in this reaction also reacts with dG to yield the OTB-dG adduct (21), which has been detected by LC-MS in the kidney of male rats fed a carcinogenic dose of OTA (22). Thus, OTB-GSH and OTHQ-GSH, along with the corresponding NAC-conjugates, were considered as appropriate biomarkers for OTA exposure. The conjugates stem from the same electrophiles that are deemed important for OTA-mediated DNA adduction (14), which is now expected to play a key role in the mutagenicity and carcinogenicity of OTA (12). However, unlike the DNA adducts generated by OTA, the GSH- and NAC-conjugates of OTA are stable to acid and can be extracted from biological tissues using strategies developed for the parent toxin (27, 29, 37). This suggested that the conjugates would be easier to detect than the corresponding DNA adducts and would still serve as an indication that the biological target (DNA) had been exposed to OTA-mediated electrophiles.

To test the potential for conjugate formation by OTA, Dark Agouti rat liver and kidney samples were analysed for levels of OTA, OTα, OTB-GSH, OTHQ-GSH, OTB-NAC, and OTHQ-NAC, using HPLC with fluorescence detection (34, 35). The rat organ samples were available from a study in which 7-week-old Dark Agouti male and female rats were fed various concentrations of OTA in wheat for a period of 28 days; similar to the protocol previously reported (27). Given that male rats are more susceptible than females to OTA-mediated carcinogenesis (7, 38), it was anticipated that the conjugate formation analysis would provide new insights into sex and organ differences in OTA-mediated metabolism, which might help explain the susceptibility of male rat kidney to OTA (39, 40).

Initially, the impact of OTA on liver and kidney weight (Figure 4) and the distribution of OTA in the lung, liver, and kidney of male and female rats (Figure 5) were analysed. The distribution study (Figure 5) showed no significant difference between males and females regarding OTA concentrations, which is in agreement with a recent study carried out by Vettorazzi et al. (41) on the distribution of OTA in male and female F344 rats. These studies suggest that other factors, such as differences in metabolism (40, 42), could explain the higher sensitivity of male rats to OTA carcinogenicity.

The HPLC data presented in Figures 6 and 7 demonstrate that differences in OTA metabolism between male and female rats and between the liver (Figure 6) and the kidney (Figure 7) do exist. In both liver and kidney the extent of OTA metabolism was greater in male than female rats. In the kidney, both sexes generate OTB-GSH as the principle metabolite. This was not the case in the liver where male rats generated appreciable quantities of OTα and OTHQ-GSH in addition to OTB-GSH (Figure 6A). The female rats also generated low levels of all three metabolites (Figure 6B). These results provide insight into the susceptibility of male rat kidney to OTA carcinogenesis. First, male rats generate higher levels of GSH-conjugates than female rats, suggesting a greater level of OTA bioactivation, which is required for DNA adduction (13, 14) and probably *in vivo* mutagenicity (12). Second, much higher levels of OTa are detected in the liver (Figure 6A) compared to the kidney (Figure 7A) and formation of OTα is a detoxification pathway for OTA (24-26), suggesting greater sensitivity of the kidney to OTA. At present, the GSH-conjugates of OTA in rat liver and kidney were characterised by HPLC with fluorescence detection using authentic samples for comparison. Future studies will focus on the use of LC-MS/MS strategies to unambiguously confirm the presence of the GSH-conjugates in the rat tissue samples. The GSH- and NAC-conjugates reported in this work will also be used as standards for the analysis of urine samples taken from animals and humans exposed to OTA.

CONCLUSION

We demonstrated that exposure of male and female rats to OTA results in the production of GSH-conjugates that have been detected using HPLC with fluorescence detection. These results suggest that OTA undergoes metabolism in rat liver and kidney to generate electrophiles that react covalently with GSH. These data add additional support to the hypothesis that differences in OTA metabolism between male and female rats provide a rationale for the sensitivity of male rat kidney to OTA carcinogenesis.

Acknowledgement

Support for this research was provided by the European Union ("Ochratoxin A-risk assessment" QLK1-2001-01614), the Region Midi-Pyrénées, the French Ministry of Research, the Association recherché centre cancer (ARC), Natural Sciences and Engineering Research Council of Canada (NSERC), the Canadian Foundation for Innovation (CFI), and the Ontario Innovation Trust Fund (OIT). The authors want to thank the health research laboratory (CIT, Evreux, France) and Goemar, Saint-Malo, France for the animal study and financial support for Delphine Canadas.

REFERENCES

1. Van der Merwe KJ, Steyn PS, Fourie L, Scott DB, Theron, JJ. Ochratoxin A, a toxic metabolite produced by *Aspergillus ochraceus* Wilh. Nature 1965;205:1112-3.
2. Pohland AE, Nesheim S, Friedman L. Ochratoxin A, a review. Pure Appl Chem 1992;64:1029-46.
3. Pfohl-Leszkowicz A, Manderville RA. Ochratoxin A: an overview on toxicity and carcinogenicity in animals and humans. Mol Nutr Food Res 2007;51:61-99.
4. Mally A, Dekant W. Mycotoxins and the kidney: modes of action for renal tumor formation by ochratoxin A in rodents. Mol Nutr Food Res 2009;53:467-78.
5. Kuiper-Goodman T, Hilts C, Billiard SM, Kiparissis Y, Richard IDK, Hayward S. Health risk assessment of ochratoxin A for all age-sex strata in a market economy. Food Addit Contam Part A Chem Anal Control Expo Risk Assess 2010;27:212-40.
6. International Agency for Research on Cancer (IARC). Ochratoxin A. In: Monographs on the evaluation of carcinogenic risks to humans. No. 56. Some naturally occurring substances: food items and constituents, heterocyclic aromatic amines and mycotoxins. Lyon; IARC; 1993. p. 489-521.
7. Boorman G, editor. National Toxicology Program. Technical Report on the Toxicology and Carcinogenesis Studies of Ochratoxin A (CAS No 303-47-9) in F344/N Rats (Gavage Studies). Natl Toxicol Program Tech Rep Ser 1989;358:1-142.
8. Stoev SD. Studies on carcinogenic and toxic effects of ochratoxin A in chicks. Toxins 2010;2:649-64.
9. Krogh P, Hald B, Pleština R, Ceović S. Balkan (endemic) nephropathy and foodborne ochratoxin A: preliminary results of a survey of foodstuffs. Acta Pathol Microbiol Scand B 1977;85:238-40.
10. Grosso F, Saïd S, Mabrouk I, Fremy JM, Castegnaro M, Jemmali M, Dragacci S. New data on the occurrence of ochratoxin A in human sera from patients affected or not by renal diseases in Tunisia. Food Chem Toxicol 2003;41:1133-40.
11. WHO Food Additives Series 47. Safety evaluation of certain mycotoxins in food [displayed 19 September 2012]. Available at http://www.inchem.org/documents/jecfa/jecmono/v47je01.htm
12. Hibi D, Suzuki Y, Ishii Y, Jin M, Watanabe M, Sugita-Konishi Y, Yanai T, Nohmi T, Nishikawa A, Umemura T. Site-specific *in vivo* mutagenicity in the kidney of *gpt* delta rats given a carcinogenic dose of ochratoxin A. Toxicol Sci 2011;122:406-14.
13. Manderville RA. A case for the genotoxicity of ochratoxin A by bioactivation and covalent DNA adduction. Chem Res Toxicol 2005;18:1091-7.
14. Pfohl-Leszkowicz A, Manderville RA. An update on direct genotoxicity as a molecular mechanism of ochratoxin A carcinogenicity. Chem Res Toxicol 2012;25:252-62.
15. Waidyanatha S, Lin PH, Rappaport SM. Characterization of chlorinated adducts of hemoglobin and albumin following administration of pentachlorophenol to rats. Chem Res Toxicol 1996;9:647-53.
16. Gillman IG, Clark TN, Manderville RA. Oxidation of ochratoxin A by an Fe-porphyrin system: model for enzymatic activation and DNA cleavage. Chem Res Toxicol 1999;12:1066-76.
17. Mally A, Zepnik H, Wanek P, Eder E, Dingley K, Ihmels H, Völkel W, Dekant W. Ochratoxin A: lack of formation of covalent DNA adducts. Chem Res Toxicol 2004;17:234-42.
18. Manderville RA, Pfohl-Leszkowicz A. Bioactivation and DNA adduction as a rationale for ochratoxin A carcinogenesis. World Mycotoxin J 2008;1:357-67.
19. Pfohl-Leszkowicz A. Ochratoxin A and aristolochic acid involvement in nephropathies and associated urothelial tract tumours. Arh Hig Rada Toksikol 2009;60:465-83.
20. Tozlovanu M, Faucet-Marquis V, Pfohl-Leszkowicz A, Manderville RA. Genotoxicity of the hydroquinone metabolite of ochratoxin A: structure-activity relationships for covalent DNA adduction. Chem Res Toxicol 2006;19:1241-7.
21. Dai J, Wright MW, Manderville RA. Ochratoxin A forms a carbon-bonded C8-deoxyguanosine nucleoside adduct: implications for C8 reactivity by a phenolic radical. J Am Chem Soc 2003;125:3716-7.
22. Mantle PG, Faucet-Marquis V, Manderville RA, Squillaci B, Pfohl-Leszkowicz A. Structures of covalent adducts between DNA and ochratoxin A: a new factor in debate about genotoxicity and human risk assessment. Chem Res Toxicol 2010;23:89-98.
23. Hadjeba-Medjdoub K, Tozlovanu M, Pfohl-Leszkowicz A, Frenette C, Paugh RJ, Manderville RA. Structure-activity

relationships imply different mechanisms of action for ochratoxin A-mediated cytotoxicity and genotoxicity. Chem Res Toxicol 2012;25:181-90.
24. Doster RC, Sinnhuber RO. Comparative rates of hydrolysis of ochratoxins A and B *in vitro*. Food Cosmet Toxicol 1972;10:389-94.
25. Stander MA, Steyn PS, van der Westhuizen FH, Payne BE. A kinetic study into the hydrolysis of the ochratoxins and analogues by carboxypeptidase A. Chem Res Toxicol 2001;14:302-4.
26. Mally A, Keim-Heusler H, Amberg A, Kurz M, Zepnik H, Mantle P, Völkel W, Hard GC, Dekant W. Biotransformation and nephrotoxicity of ochratoxin B in rats. Toxicol Appl Pharmacol 2005;206:43-53.
27. Castegnaro M, Canadas, D, Vrabcheva T, Petkova-Bocharova T, Chernozemsky IN, Pfohl-Leszkowicz A. Balkan endemic nephropathy: role of ochratoxins A through biomarkers. Mol Nutr Food Res 2006;50:519-29.
28. Duarte SC, Pena A, Lino CM. Human ochratoxin A biomarkers-from exposure to effect. Crit Rev Toxicol 2011;41:187-212.
29. Molinié A, Faucet V, Castegnaro M, Pfohl-Leszkowicz A. Analysis of some breakfast cereals on the French market for their contents of ochratoxin A, citrinin and fumonisin B_1: development of a method for simultaneous extraction of ochratoxin A and citrinin. Food Chem 2005;92:391-400.
30. Dai J, Park G, Wright MW, Adams M, Akman SA, Manderville RA. Detection and characterization of a glutathione conjugate of ochratoxin A. Chem Res Toxicol 2002;15:1581-8.
31. Brow ME, Dai J, Park G, Wright MW, Gillman IG, Manderville RA. Photochemically catalyzed reaction of ochratoxin A with D- and L-cysteine. Photochem Photobiol 2002;76:649-56.
32. Il'ichev YV, Perry JL, Manderville RA, Chignell CF, Simon JD. The pH-dependent primary photoreactions of ochratoxin A. J Phys Chem B 2001;105:11369-76.
33. Pfohl-Leszkowicz A, Tozlovanu M, Manderville R, Peraica M, Castegnaro M, Stefanovic V. New molecular and field evidences for the implication of mycotoxins but not aristolochic acid in Human Nephropathy and Urinary tract tumor. Mol Nutr Food Res 2007;51:1131-46.
34. Jennings-G JE, Tozlovanu M, Manderville R, Miller MS, Pfohl-Leszkowicz A, Schwartz GG. Ochratoxin A: In utero exposure in mice induces adducts in testicular DNA. Toxins 2010;2:1428-44.
35. Faucet-Marquis V, Pont F, Størmer F, Rizk T, Castegnaro M, Pfohl-Leszkowicz A. Evidence of a new dechlorinated OTA derivative formed in opossum kidney cell cultures after pre-treatment by modulators of glutathione pathways. Correlation with DNA adducts formation. Mol Nutr Food Res 2006;50:531-42.
36. Dais P, Stefanaki I, Fragaki G, Mikros E. Conformational analysis of ochratoxin A by NMR spectroscopy and computational molecular modeling. J Phys Chem B 2005;109:16926-36.
37. Pfohl-Leszkowicz A, Castegnaro M. Further arguments in favour of direct covalent binding of ochratoxin A (OTA) after metabolic biotransformation. Food Addit Contam 2005;22(Suppl 1):75-87.
38. Castegnaro M, Mohr U, Pfohl-Leszkowicz A, Estève J, Steinmann J, Tillman J, Michelon J, Bartsch H. Sex and strain-specific induction of renal tumours by ochratoxin A rats correlates with DNA adduction. Int J Cancer 1998;77:70-5.
39. Pfohl-Leszkowicz A, Pinelli E, Bartsch H, Mohr U, Castegnaro M. Sex and strain differences in ochratoxin A metabolism and DNA adduction in two strains of rats. Mol Carcinogen 1998;23:76-83.
40. Pfohl-Leszkowicz A, Bartsch H, Azémar B, Mohr U, Estève J, Castegnaro M. MESNA protects rats against nephrotoxicity but not carcinogenicity induced by ochratoxin A, implicating two separate pathways. Facta Universitatis Ser Med Biol 2002;9:57-63.
41. Vettorazzi A, de Trocóniz IF, Gonzalez-Peñas E, Arbillaga L, Corcuera L-A, Gil AG, de Cerain, AL. Kidney and liver distribution of ochratoxin A in male and female F344 rats. Food Chem Toxicol 2011;49:1935-42.
42. Petkova-Bocharova T, El Adlouni C, Faucet V, Pfohl-Leszkowicz A, Mantle P. Analysis for DNA adducts, ochratoxin A content and enzymes expression in kidneys of pigs exposed to mild experimental chronic ochratoxicosis. Facta Universitatis Ser Med Biol 2003;10:111-5.

Sažetak

GLUTATIONSKI KONJUGATI OKRATOKSINA A KAO BIOMARKERI IZLOŽENOSTI

U ovom je ispitivanju korištena fotoreaktivnost kancerogenog mikotoksina okratoksina A (OTA) kako bi se stvorili izvorni uzorci reduciranih glutationskih (GSH) i *N*-acetilcisteinskih (NAC) konjugata osnovnog toksina. Ovi konjugati, uz netoksični OTα, koji se stvara hidrolizom amidne veze OTA putem karboksipeptidaze A, upotrijebljeni su kao biomarkeri za ispitivanje metabolizma OTA u jetri i bubregu ženki i mužjaka štakora soja Dark Agouti. Mužjaci su se pokazali podložnijima stvaranju bubrežnih tumora uzrokovanih OTA toksinom od ženki. Utvrdili smo da se raspodjela OTA u bubrezima ženki i mužjaka značajno ne razlikuje. Međutim mužjaci su imali intenzivniji metabolizam OTA nego ženke. U jetri su utvrđene mnogo više razine OTα u usporedbi s bubregom, a rezultati upućuju na to da je stvaranje OTα detoksifikacijski put za OTA. Zaključujemo da bi se veća osjetljivost mužjaka štakora na toksičnost OTA mogla pripisati spolno uvjetovanim razlikama u njegovu metabolizmu.

KLJUČNE RIJEČI: *bioaktivacija, glutation, kancerogenost, metabolizam, mutagenost, N-acetilcistein, okratoksin A, stvaranje adukata u molekuli DNA*

CORRESPONDING AUTHOR:

Richard A. Manderville
Departments of Chemistry and Toxicology
University of Guelph
Guelph, Ontario, Canada
E-mail: *rmanderv@uoguelph.ca*